Hindawi
Shock and Vibration
Volume 2023, Article ID 8492360, 11 pages
https://doi.org/10.1155/2023/8492360

Research Article

Influence of Depth and Position of Vibration-Isolating Slot on Damping Effect of Blasting Vibration

Xiao Li,[1,2,3] **Xinquan Wang**,[2,3] **Hongguo Diao**,[2,3] **He Zhang**,[1] **and Chun Zhu**[4]

[1]*College Civil Engineering & Architecture, Zhejiang University, Hangzhou 310058, China*
[2]*Hangzhou City University, Hangzhou 310015, China*
[3]*Zhejiang Engineering Research Center of Intelligent Urban Infrastructure, Hangzhou 310015, China*
[4]*Hohai University, Nanjing 210098, China*

Correspondence should be addressed to Xinquan Wang; wangxq@zucc.edu.cn

Received 1 October 2022; Revised 4 November 2022; Accepted 24 November 2022; Published 25 February 2023

Academic Editor: Gang Wang

The blasting vibration has an impact on the rock and soil around the blasting hole and the nearby structures. The vibration-isolating slot is one of the methods to reduce the damage of blasting vibration. In this paper, the influences of the depth and position of the vibration isolation slot on the PPV (peak particle velocity) attenuation characteristics of the ground vibration and blasting vibration damping effect of the vibration isolation slot at different measuring points are studied systematically by LS-DYNA numerical models. The results show that the damping effect of the vibration isolation slot is realized by reflecting the blasting vibration wave and increasing the propagation paths of the blasting vibration wave. When the measuring points are 5 m~45 m far away from the vibration-isolating slot, the average vibration damping effect of the vibration-isolating slot is more than 30% and the deeper the depth of the vibration isolation slot, the better the vibration damping effect when the measuring points are 5 m~15 m far away from the vibration isolation slot. However, when the measuring points are 15 m~45 m far away from the vibration isolation slot, the vibration damping effect is best when the depth of the vibration isolation slot is 15 m. The vibration damping effect of blasting vibration at the same measuring point is different due to different positions of vibration isolation slot. For the measuring points M_3 and M_5, with the increasing of the distance between the vibration-isolating slot and the explosion source, the vibration damping effect of the vibration-isolating slot shows an increasing-decreasing-increasing trend; however, it shows a decreasing-increasing-decreasing trend for the measuring point M_4.

1. Introduction

Engineering blasting technology is widely used in various fields such as mining, tunnel boring, road rift excavation, and building demolition due to its advantages of high efficiency, economy, and ease of operation [1–5]. Explosive explosion in rock mass will generate huge energy, which will not only cause rock breaking but also cause damage to adjacent structures due to the negative effects of blasting vibration, such as building cracking, coal mine roadway rock burst, and surrounding rock block sliding [6–11]. For example, building cracking damage that occurred in Çatakköprü and Susuz villages in Silvan district of Diyarbakır, Turkey [10], and the coal mine rock burst damage that occurred in Hegang mining area, China [11], are all related to rock blasting. How to control the blasting vibration has become one of the focus problems in blasting construction.

Through the study of the propagation characteristics of blasting vibration wave, the engineering community has taken many vibration reduction measures to control the damage caused by blasting vibration. Because of the good damping effect and the convenience and economy of construction, the vibration-isolating slot has been widely used in blasting construction. At present, many scholars have studied the damping mechanism and damping effect of the vibration-isolating slot. In the research of damping mechanism, Schoneberg [12] studied the interaction between the linear sliding medium surface and the stress wave and found

that the stress wave would be reflected and diffracted when passing through the precrack surface. Song et al. [13, 14] and Luo et al. [15] investigated the wave propagation characteristics and dynamic failure characteristics of jointed rock mass. They obtained that rock joints hinder wave propagation and are more likely to cause rock failure. Haupt [16, 17] carried out a variety of model experiments with vibration isolation effect on the ground, including open ditches and underground concrete walls, and pointed out that the scattering effect is only related to the cross-sectional area of the vibration isolation barrier, not its actual shape. Through numerical simulation of bench blasting, Yu et al. [18] concluded that the vibration-isolating slot weakens the body wave by concentrating the energy of the body wave first. Lu et al. [19] studied the interaction between explosive stress wave and precrack with the interface model described by joint stiffness. Through model calculation and analysis, it is concluded that the precrack has high-frequency filtering effect on the incident explosion stress wave, and the precrack should be ensured to have sufficient width to prevent it from closing under the action of the incident explosion stress wave. Hu et al. [20] showed the propagation path of blasting stress wave in the precrack by numerical simulation and described the influence of boundary surface on the propagation of blasting stress wave by generating von Mises stress cloud. In the research of damping effect, Woods [21] performed a series of scaled field experiments on vibration isolation by installing open trenches very close to the wave source (known as active isolation) as well as near the machine or structure to be protected (known as passive isolation). In the study, the ratio of the amplitude of the vibration in the isolation area to the amplitude of the vibration in the isolation area without the isolation trench is used as an index to evaluate its vibration reduction function. Çelebi et al. [22] explored the vibration reduction effect of the empty trench and the filled trench through the harmonic load generated by the electric vibrator and concluded that the vibration reduction effect of the empty trench is better than that of the filled trench. However, due to its own instability, the depth of the empty ditch is greatly limited. The filling materials of the filling ditch include water, mottled clay, and concrete. Through comparison, it is found that the softer the filling material, the better the vibration reduction effect, and the passive vibration isolation is better than the active vibration isolation. By numerical simulations, Berzal [23] found that if two damping ditches are set in the blasting area, the damping rate is higher than that of only one damping ditch. Tang et al. [24] simulated the propagation characteristics of blasting vibration wave in concave landform based on UDEC (Universal Distinct Element Code) program and concluded that concave landform has obvious attenuation effect on blasting vibration wave, and the attenuation amplitude of horizontal vibration velocity is greater than that of vertical vibration velocity. At the same time, the attenuation coefficient increases with the increase of the depth and width of the concave landform, but the amplitude with the increase of the width is small. Prakash et al. [25] conducted experiments on the impact of slot depth on the vibration-isolating rate. The ratio of slot depth and pore depth was 0.3, 1.0, and 1.125, and the vibration-isolating rate was 16.6–55%. Venkatesh [26] studied the peak vibration velocity of the particles on both sides of the slot when the depth of the vibration-isolating slot was more than the hole depth and obtained the vibration-isolating rate between 11 and 18.5%.

The above research studies are of great significance to the safety control of adjacent structures under blasting vibration. However, the influence of the depth and position of the vibration isolation slot on the damping effect of blasting vibration is not studied systematically. For example, what is the attenuation degree of ground vibration at different distances from the vibration isolation slot ? With the continuous construction of infrastructure, there are more and more blasting construction projects in cities and vibration isolation slots are often set to ensure the safety of multiple structures. However, the distance between these structures and the explosion source may be different, and their blasting vibration sensitivity may also be different. Therefore, it is also necessary to specifically analyze the damping effect of the vibration isolation slot on the measuring points at different positions from the explosion source. In this paper, the influences of the depth and position of the vibration isolation slot on the attenuation characteristics of the ground vibration at different measuring points are studied systematically by LS-DYNA numerical simulations.

2. Computational Models

2.1. Computational Analysis Models. In order to systematically study the influences of the depth and position of the vibration isolation slot on the attenuation characteristics of the ground vibration at different measuring points, a series of LS-DYNA models are established, as shown in Figure 1. The whole size of the models is 50 m × 100 m. The location of the explosion source is fixed, and the distances between the measuring points (M_1, M_2, M_3, M_4, and M_5) and the explosion source are also fixed. Generally, the propagation and attenuation of blasting vibration in the range of tens of meters is fast, so the distance between the measuring point and the vibration-isolating slot studied in this paper is 5 m~45 m. The charge diameter and the height of all the models are the same and are 150 mm × 1 m. The diameter and the height of the blast hole are 150 mm × 6 m, which are fixed. The charge quantity and charge form of each blasting are consistent. The widths of the vibration isolation slot of all models are uniform, 0.5 m. Figure 1(a) shows the comparative reference model without vibration-isolating slot. Figure 1(b) shows the analysis models with various vibration-isolating slot depths. The depths H of these models are 5 m, 10 m, 15 m, and 20 m. The horizontal distance distance L between the blasting source and the vibration-isolating slot is fixed as 5 m. Figure 1(c) shows the analysis models with various vibration-isolating slot positions. The horizontal distance L between the blasting source and the vibration-isolating slot of these models is 5 m, 10 m, 15 m, and 20 m. The depth of the vibration-isolating slot is fixed as 10 m.

The element size of the finite element model is 0.25 m. The translation and rotational degrees of freedom of the

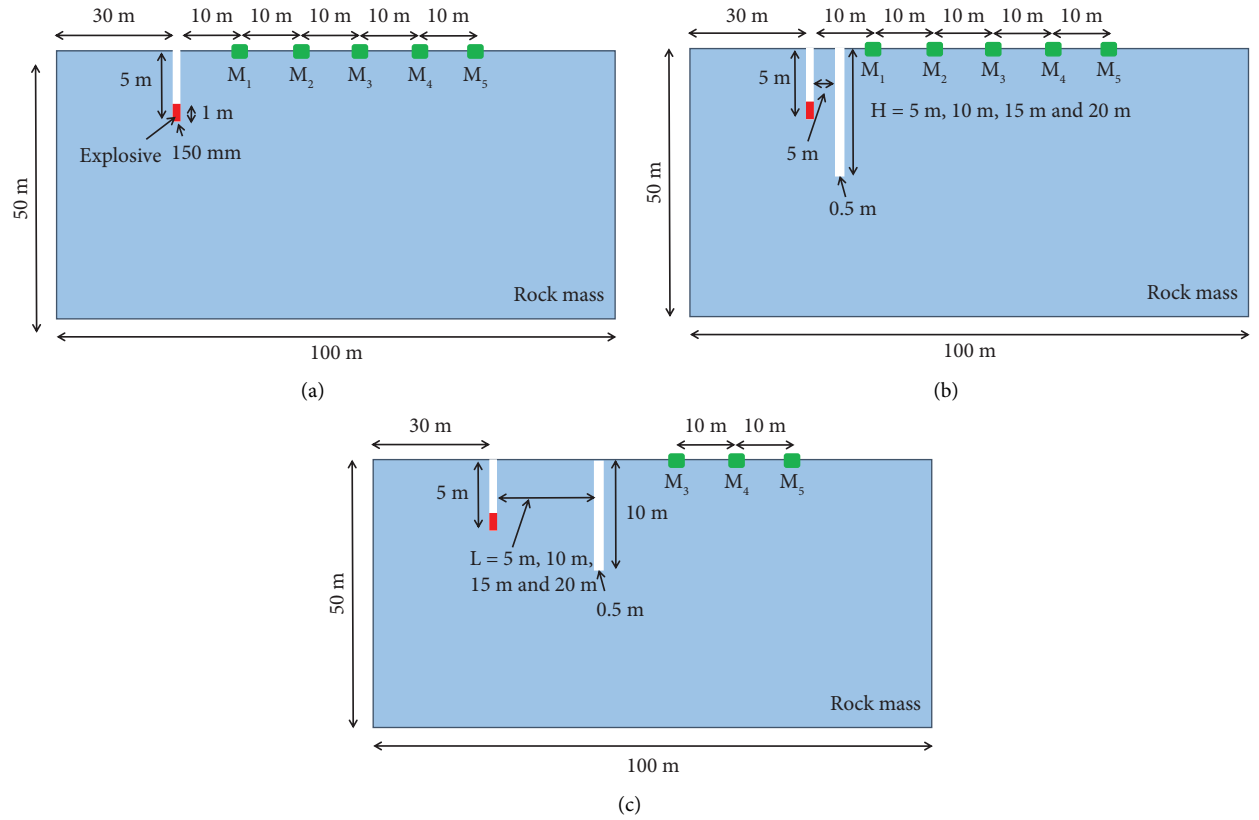

Figure 1: Computational analysis models. (a) Comparative reference model without vibration-isolating slot. (b) Analysis models with various vibration-isolating slot depths. (c) Analysis models with various vibration-isolating slot positions.

nodes at the bottom of the model are constrained; the nonreflective boundary effect is considered. Except for the top free surface of the model, all nodes on the outer boundary of the model are set with a non reflective boundary. The unit system used in this paper is m-kg-s.

2.2. Constitutive Models of Materials

2.2.1. Constitutive Model of TNT Explosive. TNT (trinitrotoluene) explosive is generally used for surface foundation blasting excavation [27]. The TNT explosive can be simulated by the equation of state (EOS) in LS-DYNA [28]. The EOS of the JWL (Jones–Wilkins–Lee) has been widely used to simulate the relationship between pressure and specific volume in the explosion process [27, 28]. The JWL equation is written as

$$P = A\left(1 - \frac{\omega}{R_1 V}\right)e^{-R_1 V} + B\left(1 - \frac{\omega}{R_2 V}\right)e^{-R_2 V} + \frac{\omega E}{V}, \quad (1)$$

where A, B, R_1, R_2, and ω are material constants for TNT explosive, A and B represent the magnitudes of pressure, ρ is the density of the explosive, and E is the specific internal energy at atmospheric pressure. Referring to the research studies conducted by Zhang et al. [27] and Tiwari et al. [28], the physical and mechanical parameters of the TNT explosive in the simulation are listed in Table 1.

Table 1: Parameters of the TNT explosive material model [27, 28].

ρ (kg/m^3)	Detonation velocity (m/s)	A (GPa)	B (GPa)	R_1	R_2	ω
1630	6930	373.8	3.747	4.15	0.9	0.35

2.2.2. Constitutive Model of Air. The air model is usually described by keyword *MAT_NULL combined with multilinear equation of state *EOS_LINEAR_POLYNOMIAL in this study [20]:

$$P = \left[C_0 + C_1\mu + C_2\mu^2 + C_3\mu^2\right] + \left[C_4 + C_5\mu + C_6\mu^2\right] \cdot e. \quad (2)$$

For the convenience of calculation, air is regarded as an ideal gas, in which the parameters are as follows [23]: $C_0 = C_1 = C_2 = C_3 = C_6 = 0$ and $C_4 = C_5 = 0.4$. For air, the parameters of the null material model are as follows: density $\rho = 1.2\,\text{kg/m}^3$ and dynamic viscosity coefficient $u = 0.001$.

2.2.3. Constitutive Model of Rock Mass. In this paper, the rock is simulated by means of the Drucker–Prager model, which is usually used for simulations of rock masses in LS-DYNA [27, 28]. The yield criteria of the Drucker–Prager model are given by

$$F = \frac{q}{2}\left[1 + \frac{1}{K} - \left(1 - \frac{1}{K}\right)\left(\frac{r}{q}\right)^3\right] - p' \tan\beta - d = 0, \quad (3)$$

where q represents the deviatoric stress [$= \sqrt{3/2}\sqrt{Sij{:}\ Sij}$], Sij represents the deviatoric stress tensor, p' represents the mean stress $= (\sigma_1' + \sigma_2' + \sigma_3')/3$, K is a scalar parameter that determines the shape of the yield surface and maintains the convexity of the yield surface in the deviatoric (π) plane, and r is the third invariant of the deviatoric stress tensor. The parameter β is related to the angle of internal friction φ at the stage of no dilatancy (the critical state of sand) using a correlation given by

$$\tan\beta = \frac{\sqrt{3}\sin\phi}{\sqrt{1 + (1/3)\sin^2\phi}}. \quad (4)$$

d is the hardening parameter related to cohesion, and c is through a correlation given by

$$\frac{d}{c} = \frac{\sqrt{3}\cos\phi}{\sqrt{1 + (1/3)\sin^2\phi}}. \quad (5)$$

In this paper, the slightly to moderately quartzite rock mass is used for built models, and the properties of quartzite rock mass are given in Table 2 [28].

Table 2: Properties of quartzite rock mass [28].

Parameters	Values
Specific gravity (G)	2.65
Density (ρ) (kg/m^3)	2550
Elastic modulus (E) (GPa)	28
Poisson's ratio (ν)	0.25
Angle of internal friction (φ)	45°
In situ stress ratio (K_0)	0.5
Dilation angle (ψ)	5°
Cohesion (c) (MPa)	2.3
σ_c (MPa)	40

3. Analysis of Computational Results

3.1. Ground Vibration of Blasting without Vibration-Isolating Slot. Figure 2 shows the resultant velocity ($V = \sqrt{(V_x^2 + V_y^2 + V_z^2)}$) cloud atlas of blasting vibration propagation in rock mass without the vibration-isolating slot. It can be seen from the figures that the explosive diffuses outward in the form of spherical wave after blasting in the blast hole. When the blasting vibration wave reaches the ground surface, the reflection of the blasting vibration wave will occur, and the reflected wave will be superposed with the incident wave. This implies that the ground vibration is the common response of complex blasting vibration wave superposition.

Figure 3 shows the resultant velocity time histories and PPV of ground vibration of blasting without the vibration-isolating slot. As can be seen from Figure 3(a), the farther the measuring point from the blast source, the smaller the peak of the blasting vibration resultant velocity (PPV). Currently, the empirical model of the following form [29] is widely used to predict blast vibration PPV:

$$\begin{aligned} \mathrm{PPV} &= k \cdot \mathrm{SD}^{-\beta} \\ &= k \cdot \left(\frac{R}{Q^{1/3}}\right)^{-\beta}, \end{aligned} \quad (6)$$

where k and β are the site coefficient and attenuation coefficient; R is the space distance between the measuring point and the explosion source; and Q is the explosive quantity. From Figure 3(b), it can be seen that the empirical equation (6) can effectively predict the blast vibration PPV when the blasting is without the effect of vibration-isolating slot.

3.2. Influence of Vibration-Isolating Slot Depths and Positions on Ground Vibration. Here, we take the computational model with vibration isolation slot with a depth of 5 m and a distance of 5 m from the explosion source as an example to explore the damping mechanism of the vibration-isolating slot. As shown in Figure 4(a), when the blasting vibration wave does not encounter the vibration isolation slot, the blasting vibration wave still diffuses outward in the form of spherical wave. At this time, the characteristics of blasting vibration are consistent with the computational model without vibration isolation slot (as shown in Figure 2(a)). When the blasting vibration wave meets the vibration-isolating slot, the blasting vibration wave will be reflected and diffracted, as shown in Figures 4(b)–4(d). From these figures, it can be seen that the superposition of blasting vibration waves generated on the side of the isolation slot towards blasting source will produce greater amplitude; on the side far away from the blasting source, the amplitude of blasting vibration wave is blocked by the isolation slot, and the amplitude is relatively small. At this time, part of the energy of blasting vibration wave is reflected back by the vibration isolation slot, and the other part is diffracted from the bottom of the vibration isolation slot to the rock behind, which will greatly weaken the energy of the blasting vibration. Therefore, the damping effect of the vibration isolation slot is realized by reflecting the blasting vibration wave and increasing the propagation paths of the blasting vibration wave.

Figure 5 shows the resultant velocity time histories and PPV of ground vibration of blasting with a vibration-isolating slot with a depth of 5 m and a distance of 5 m from the explosion source. Comparing Figures 5(a) and 3(a), it can be seen that due to the effect of the blasting vibration isolation slot, the blasting vibration resultant velocity of the rock mass behind the vibration isolation slot has been greatly attenuated. In addition, the vibration velocity of the measuring point M_1 is not the largest, mainly because the measuring point M_1 is close to the vibration isolation slot, and the diffraction and scattering of the blasting vibration wave during the propagation to the measuring point M_1 increase, which dissipates large energy.

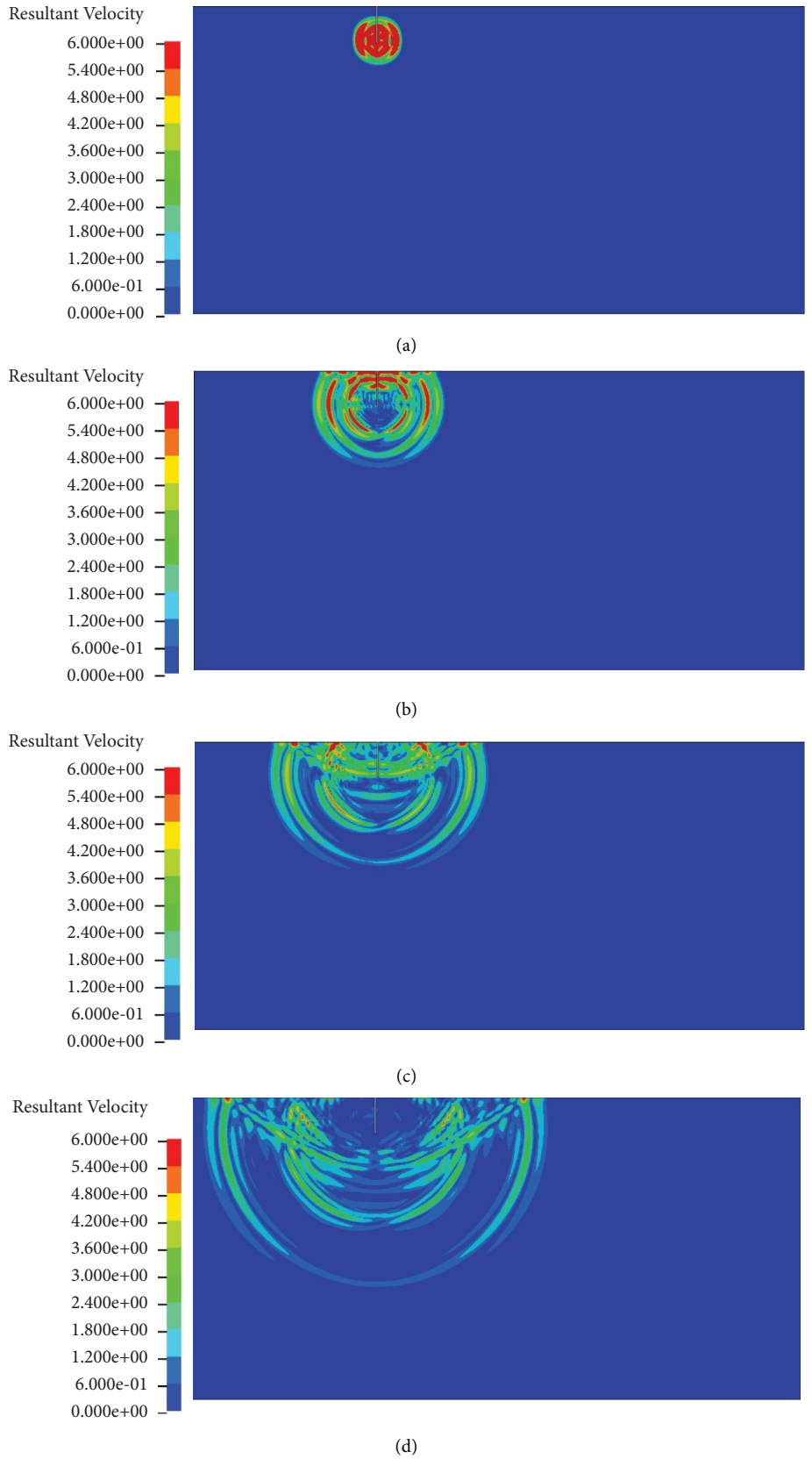

Figure 2: Propagation characteristics of vibration resultant velocity without vibration-isolating slot. (a) Time = 1 ms. (b) Time = 3 ms. (c) Time = 5 ms. (d) Time = 8 ms.

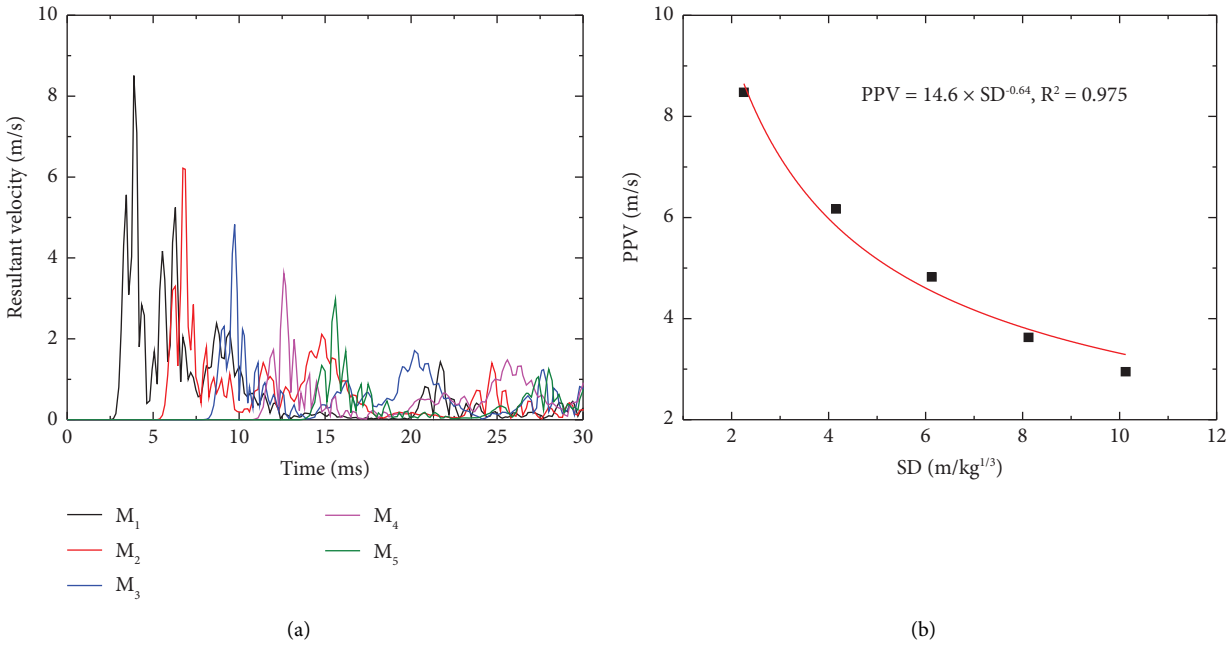

Figure 3: Resultant velocity time histories and PPV of ground vibration induced by blasting without vibration-isolating slot. (a) Resultant velocity time histories. (b) PPV.

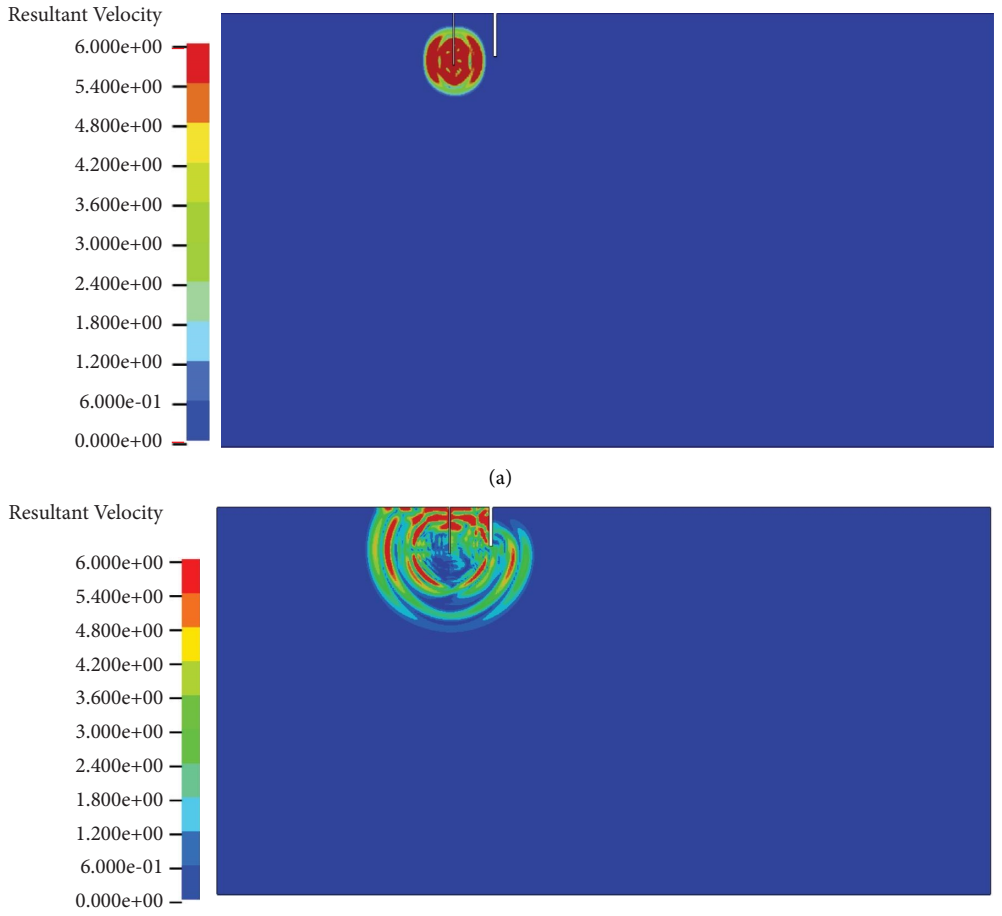

Figure 4: Continued.

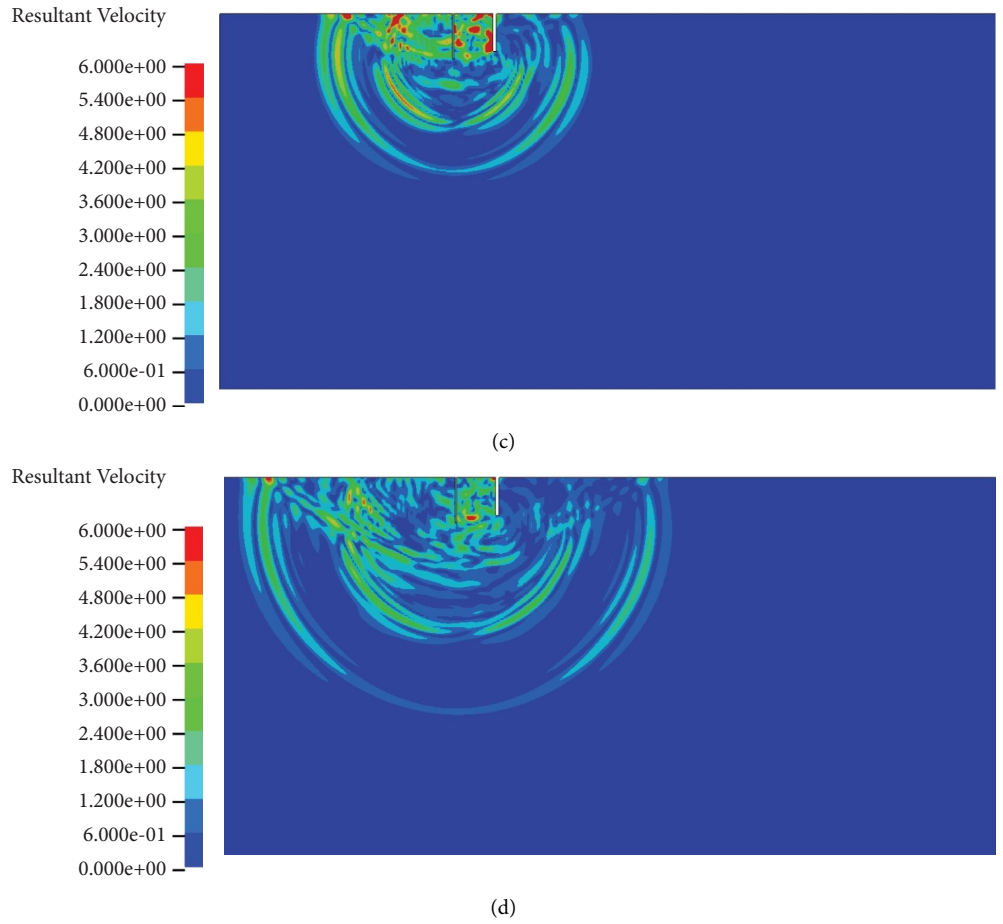

Figure 4: Propagation characteristics of vibration resultant velocity with a vibration-isolating slot. (a) Time = 1 ms. (b) Time = 3 ms. (c) Time = 5 ms. (d) Time = 8 ms.

It can be seen from Figure 5(b) that due to the influence of the vibration isolation slot, the blasting vibration PPV does not completely decrease with the increase of the distance from blasting source. The PPV of blasting vibration tends to increase first at the position near to the vibration isolation slot. In addition, the empirical equation (6) is less effective in predicting the PPV of blast vibration when the propagation of the blasting vibration propagates through a vibration isolation slot.

In summary, the vibration isolation slot has an important influence on the attenuation of blast vibration wave propagation. Next, we analyze the effect of different depths and locations of vibration isolation slots on the damping effect of blasting at different test locations. In this study, the ratio of the amplitude (As) of the vibration in the measuring points behind the vibration isolation slot to the amplitude (A) of the vibration in the measuring points in the same position without the vibration isolation slot is used as an index to evaluate its vibration reduction function:

$$\zeta = 1 - \frac{As}{A}, \tag{7}$$

where ζ is the attenuation coefficient of blasting vibration wave.

3.2.1. Influence of Vibration-Isolating Slot Depths. Figure 6 shows the PPV on measuring points of blasting with a vibration-isolating slot with different depths. It can be seen from the figure that the attenuation of blasting vibration wave behind the vibration-isolating slot increases first and then decreases, mainly because the closer to the vibration-isolating slot, the more obvious the diffraction and scattering phenomenon. When the measuring point is close to the vibration-isolating slot, e.g., within the range of 5 m~15 m, the blasting vibration PPV tends to decrease gradually with the increase of the depth of the vibration-isolating slot. However, when the distance between the measuring point and the vibration-isolating slot is more than 15 m, the blasting vibration PPV increases first and then decreases with the increase of the depth of the vibration-isolating slot. The main reason is that the blasting vibration wave will be reflected on the ground surface, and the superposition of reflected wave and incident wave is different.

Figure 7 shows attenuation coefficient of blasting vibration wave of blasting with a vibration-isolating slot with different depths. It can be seen from the figure that the vibration-isolating slot has good vibration damping effect. Within the range of 5 m~45 m between the measuring point and the vibration-isolating slot, the average vibration

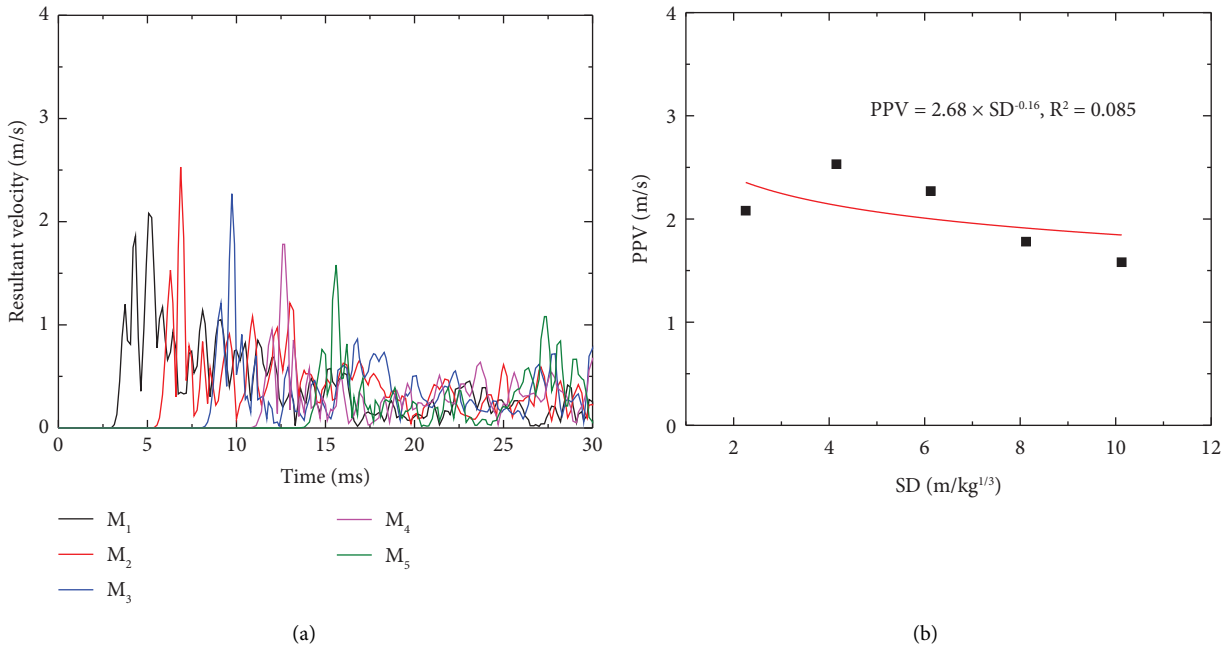

Figure 5: Resultant velocity time histories and PPV of ground vibration induced by blasting with a vibration-isolating slot. (a) Resultant velocity time histories. (b) PPV.

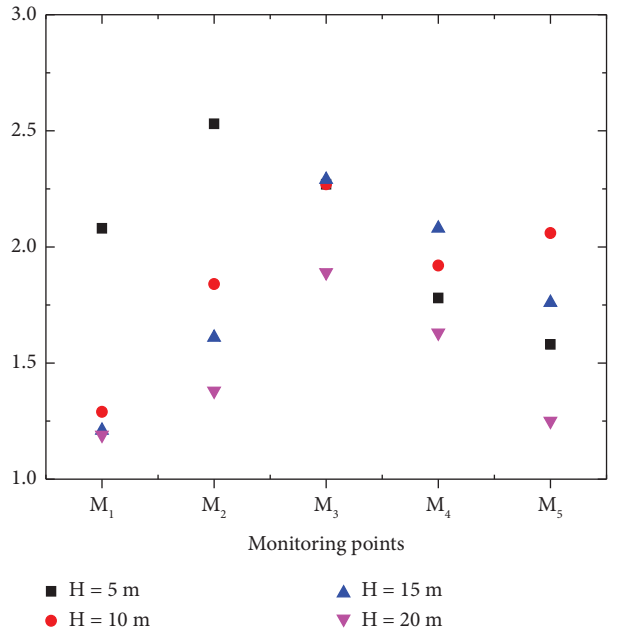

Figure 6: PPV on measuring points of blasting with a vibration-isolating slot with different depths.

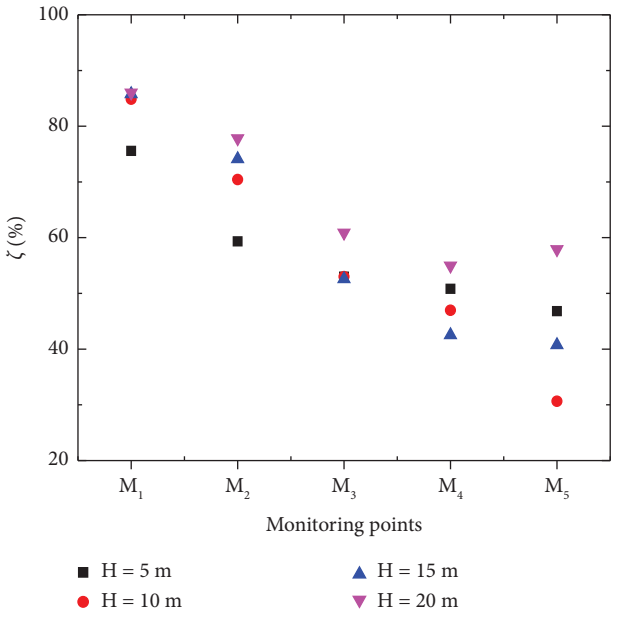

Figure 7: Attenuation coefficient of blasting vibration wave of blasting with a vibration-isolating slot with different depths.

damping effect of the vibration-isolating slot is more than 30%. Generally, the vibration damping effect of the vibration-isolating slot is better for the measuring points closer to the vibration-isolating slot. With the increase of the depth of the vibration-isolating slot, the vibration damping effect gradually increases within the range of 5 m~15 m between the measuring points and the vibration-isolating slot. However, when the distance between the measuring points and the vibration isolation slot is relatively larger, the increase of the depth of the vibration isolation slot does not necessarily lead to the attenuation of the blasting vibration PPV. Within the range of 5 m~15 m from the measuring points to the vibration isolation slot, the deeper the depth of the vibration isolation slot, the better the vibration damping effect. Within the range of 15 m~45 m from the measuring point to the vibration isolation slot, the vibration damping effect is best when the depth of the vibration isolation slot is 15 m.

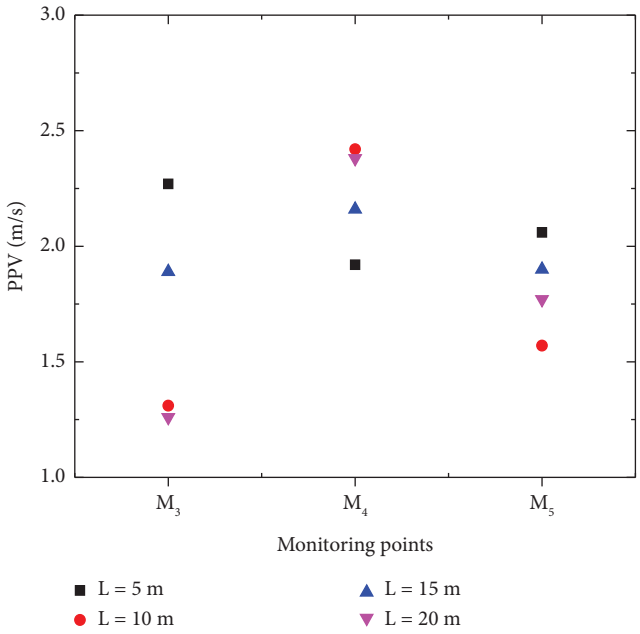

Figure 8: PPV on measuring points of blasting with a vibration-isolating slot with different positions.

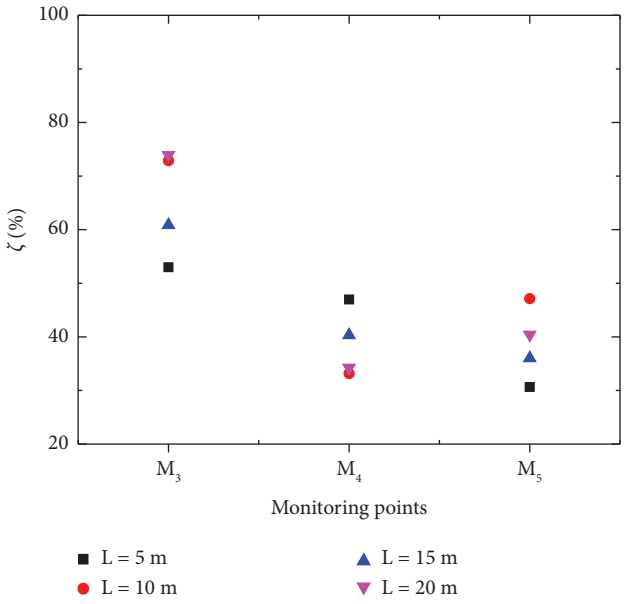

Figure 9: Attenuation coefficient of blasting vibration wave of blasting with a vibration-isolating slot with different positions.

3.2.2. Influence of Vibration-Isolating Slot Positions. Since the measuring points M_1 and M_2 are located in front of the vibration-isolating slot when the distance between the vibration-isolating slot and the explosion source is 20 m, the PPV characteristics of the blasting vibration of the measuring points M_1 and M_2 and the vibration damping effect of the vibration-isolating slot for the measuring points M_1 and M_2 will not be discussed in this section. Figure 8 shows the PPV on measuring points of blasting with a vibration-isolating slot with different positions. It can be seen from the figure that the blasting vibration PPV characteristics at the same measuring point are different with different positions of vibration-isolating slot. For the measuring points M_3 and M_5, with the increase of the distance between the vibration-isolating slot and the blasting source, the blasting vibration PPV shows a decreasing-increasing-decreasing trend, and the PPV is the largest when $L = 5$ m. However, for the measuring point M_4, with the increase of the distance between the vibration-isolating slot and the blasting source, the blasting vibration PPV shows a increasing-decreasing-increasing trend, and the PPV is the largest when $L = 10$ m.

Figure 9 shows attenuation coefficient of blasting vibration wave of blasting with a vibration-isolating slot with different positions. It can be seen from the figure that the vibration damping effect of blasting vibration at the same measuring point is different due to different positions of vibration-isolating slots. It can be seen from the figure that different positions of vibration-isolating slot have different effects on the vibration damping effect of the same measuring point. For the measuring point M_3, with the increasing distance between the vibration-isolating slot and the explosion source, the vibration damping effect of the vibration-isolating slot shows an increasing-decreasing-increasing trend, and the vibration damping effect is the best when $L = 20$ m. For the measuring point M_4, with the increasing distance between the vibration-isolating slot and the explosion source, the vibration damping effect of the vibration-isolating slot shows a decreasing-increasing- decreasing trend, and the vibration damping effect is the best when $L = 5$ m. For the measuring point M_5, with the increasing distance between the vibration-isolating slot and the explosion source, the vibration damping effect of the vibration-isolating slot shows an increasing-decreasing-increasing trend, and the vibration damping effect is the best when $L = 10$ m.

4. Conclusions

In this paper, the influences of the depth and position of the vibration isolation slot on the PPV attenuation characteristics of the ground vibration and blasting vibration damping effect of the vibration isolation slot at different measuring points are studied systematically by LS-DYNA numerical simulation models, and some useful conclusions are obtained.

The ground vibration is the common response of complex blasting vibration wave superposition. Without the influence of vibration isolation trench, the PPV of blasting vibration will decrease with the increase of the distance between the measuring point and the explosion source.

The damping effect of the vibration isolation slot is realized by reflecting the blasting vibration wave and increasing the propagation paths of the blasting vibration wave. Due to the influence of the vibration isolation slot, the blasting vibration PPV does not completely decrease with the increase of the distance from blasting source. The PPV of blasting vibration tends to increase first at the position near to the vibration isolation slot.

Within the range of 5 m~45 m between the measuring point and the vibration-isolating slot, the average vibration damping effect of the vibration-isolating slot is more than 30%. Generally, the vibration damping effect of the vibration-isolating slot is better for the measuring points closer to the vibration-isolating slot.

Within the range of 5 m~15 m from the measuring points to the vibration isolation slot, the deeper the depth of the vibration isolation slot, the better the vibration damping effect. Within the range of 15 m~45 m from the measuring point to the vibration isolation slot, the vibration damping effect is best when the depth of the vibration isolation slot is 15 m.

The vibration damping effect of blasting vibration at the same measuring point is different due to different positions of isolation vibration isolation slot. For the measuring points M_3 and M_5, with the increasing distance between the vibration-isolating slot and the explosion source, the vibration damping effect of the vibration-isolating slot shows an increasing-decreasing-increasing trend. However, for the measuring point M_4, with the increasing distance between the vibration-isolating slot and the explosion source, the vibration damping effect of the vibration-isolating slot shows a decreasing-increasing-decreasing trend.

Data Availability

The data used to support the findings of this study are included within the article.

Conflicts of Interest

The authors declare that they have no conflicts of interest.

Acknowledgments

This research was funded by National Natural Science Foundation of China (52109139 and 52009122), China Postdoctoral Science Foundation (2022M712724), and Natural Science Foundation of Zhejiang Province (LQ20E080022 and LQ21E090002).

References

[1] D. Jahed Armaghani, E. Tonnizam Mohamad, M. Hajihassani, S. V. Alavi Nezhad Khalil Abad, A. Marto, and M. R. Moghaddam, "Evaluation and prediction of flyrock resulting from blasting operations using empirical and computational methods," *Engineering with Computers*, vol. 32, no. 1, pp. 109–121, 2016.

[2] P. Pal Roy, "Emerging trends in drilling and blasting technology: concerns and commitments," *Arabian Journal of Geosciences*, vol. 14, Article ID 652, 2021.

[3] Q. Wang, M. He, S. Li et al., "Comparative study of model tests on automatically formed roadway and gob-side entry driving in deep coal mines," *International Journal of Mining Science and Technology*, vol. 31, no. 4, pp. 591–601, 2021.

[4] Q. Wang, B. Jiang, S. Xu et al., "Roof-cutting and energy-absorbing method for dynamic disaster control in deep coal mine," *International Journal of Rock Mechanics and Mining Sciences*, vol. 158, Article ID 105186, 2022.

[5] Q. Wang, S. Xu, Z. Xin, M. He, H. Wei, and B. Jiang, "Mechanical properties and field application of constant resistance energy-absorbing anchor cable," *Tunnelling and Underground Space Technology*, vol. 125, Article ID 104526, 2022.

[6] X. Wang, J. Li, X. Zhao, and Y. Liang, "Propagation characteristics and prediction of blast-induced vibration on closely spaced rock tunnels," *Tunnelling and Underground Space Technology*, vol. 123, Article ID 104416, 2022.

[7] Y. Bao, J. Chen, L. Su, W. Zhang, and J. Zhan, "A novel numerical approach for rock slide blocking river based on the CEFDEM model: a case study from the Samaoding paleolandslide blocking river event," *Engineering Geology*, Article ID 106949, 2022.

[8] S. Tang, J. Li, S. Ding, and L. Zhang, "The influence of water-stress loading sequences on the creep behavior of granite," *Bulletin of Engineering Geology and the Environment*, vol. 81, Article ID 482, 2022.

[9] X. Liang, S. Tang, C. A. Tang, L. Hu, and F. Chen, "Influence of water on the mechanical properties and failure behaviors of sandstone under triaxial compression," *Rock Mechanics and Rock Engineering*, pp. 1–32, 2022.

[10] M. E. Oncu, B. Yon, O. Akkoyun, and T. Taskiran, "Investigation of blast-induced ground vibration effects on rural buildings," *Structural Engineering & Mechanics*, vol. 54, no. 3, pp. 545–560, 2015.

[11] G. Li, *Fracturing and Dynamic Response of Low and Thick Stratas of Hard Rocks*, Shandong University of Science and Technology, Qingdao, China, 2016.

[12] M. Schoenberg, "Transmission and reflection of plane waves at an elastic-viscoelastic interface," *Geophysical Journal International*, vol. 25, no. 1-3, pp. 35–47, 1971.

[13] L. Song, Q. Jiang, Z. Zhong et al., "Technical path of model reconstruction and shear wear analysis for natural joint based on 3D scanning technology," *Measurement*, vol. 188, Article ID 110584, 2022.

[14] L. Song, G. Wang, X. Wang et al., "The influence of joint inclination and opening width on fracture characteristics of granite under triaxial compression," *International Journal of Geomechanics*, vol. 22, no. 5, Article ID 04022031, 2022.

[15] Y. Luo, G. Wang, X. Li et al., "Analysis of energy dissipation and crack evolution law of sandstone under impact load," *International Journal of Rock Mechanics and Mining Sciences*, vol. 132, Article ID 104359, 2020.

[16] W. A. Haupt, "Isolation of vibrations by concrete core walls," in *Proceedings of the 9th international conference on soil mechanics and foundation engineering*, vol. 2, pp. 251–256, Tokyo, Japan, July 1977.

[17] W. A. Haupt, "Model tests on screening of surface waves," in *Proceedings of the 10th International Conference on Soil Mechanics and Foundation Engineering*, pp. 215–222, Stockholm, Sweden, June 1981.

[18] D. Y. Yu, J. Yang, and M. S. Zhao, "Study on the absorption mechanism of damping bitch to the vibration wave in bench blasting," *Journal of China Coal Society*, vol. 36, no. 2, pp. 244–247, 2011.

[19] W. B. Lu, S. X. Lai, and Z. H. Dong, "Analysis of vibration isolating effect of pre-splitting crack in rock excavation by blasting," *Explosion and Shock Waves*, vol. 17, pp. 193–198, 1997.

[20] J. Hu, T. Lei, K. Zhou, and Q. F. Chen, "Effect of blasting vibration on pre-splitting crack in filling-environment," *Journal of Central South University*, vol. 42, no. 6, pp. 1704–1709, 2011.

[21] R. D. Woods, "Screening of surface wave in soils," *Journal of the Soil Mechanics and Foundations Division*, vol. 94, no. 4, pp. 951–979, 1968.

[22] E. Çelebi, S. Fırat, G. Beyhan, İ. Çankaya, İ. Vural, and O. Kırtel, "Field experiments on wave propagation and vibration isolation by using wave barriers," *Soil Dynamics and Earthquake Engineering*, vol. 29, no. 5, pp. 824–833, 2009.

[23] R. L. Berzal, "Blasting vibration levels transmitted across fracture planes," *Mining Magazine*, vol. 9, pp. 361–363, 1976.

[24] H. Tang, H. B. Li, Q. C. Zhou, J. R. Li, X. Xia, and L. Q. Zhang, "Numerical simulation of influence of concave landform on blasting vibration wave propagation," *Rock and Soil Mechanics*, vol. 29, no. 6, pp. 1540–1544, 2008.

[25] A. J. Prakash, P. Palroy, and D. D. Misra, "Analysis of blast vibration characteristics across a trench and a pre-split plane," *Fragblast*, vol. 8, no. 1, pp. 51–60, 2004.

[26] H. S. Venkatesh, "Influence of explosive charge on blast vibrations in surface mines," Mangalore University, Konaje, India, 2002.

[27] P. Zhang, J. Cai, F. Zong, Y. He, and Q. Wang, "Dynamic response analysis of underground double-line tunnel under surface blasting," *Shock and Vibration*, vol. 2021, Article ID 9226615, 13 pages, 2021.

[28] R. Tiwari, T. Chakraborty, and V. Matsagar, "Dynamic analysis of tunnel in weathered rock subjected to internal blast loading," *Rock Mechanics and Rock Engineering*, vol. 49, no. 11, pp. 4441–4458, 2016.

[29] Z. Zhang, C. Zhou, A. Remennikov, T. Wu, S. Lu, and Y. Xia, "Dynamic response and safety control of civil air defense tunnel under excavation blasting of subway tunnel," *Tunnelling and Underground Space Technology*, vol. 112, Article ID 103879, 2021.